Kurt Scheerschmidt, Volker Kuhlmann
Max Planck Institute of Microstructure Physics

Relaxation of semiconductor nanostructures using molecular dynamics with analytic bond order potentials*

Dedicated to Professor Dr. Hellmut Fischmeister on the occasion of his 80th birthday

Molecular dynamics simulations using empirical potentials have been performed to describe atomic interactions during the relaxation of nanostructures. To include the quantum mechanical nature of atomic bonding a tight-binding based bond order potential is developed applying analytically the first six moments. The bond order potential is improved using new on-site and π-terms of the local density of states. The applicability of the bond order potential and resulting enhancements in structural predictions are analyzed recalculating quantum dot relaxations and interface defects arising during bonding of two wafers with twist rotation misalignment. The most important property proposed by the extended bond order potential is an increased stiffness of the bonds which give modifications of local atomic arrangements near defects.

Keywords: Molecular dynamics; Bond order potential; Nanostructures; Quantum dots; Wafer bonding

1. Introduction

Molecular dynamics (MD) simulations [2] have been performed to study atomic processes related to the reordering at interfaces [3] and relaxation of nanostructures [4]. To enhance MD, we use the bond order potential (BOP) based on the tight binding (TB) model, as it preserves the essential quantum mechanical nature of atomic bonding. Just like ab initio methods, TB calculations require complete diagonalisation of the Hamiltonian, which scales as $\mathcal{O}(N^3)$ and restricts simulations to a few thousand atoms. The analytic BOP, however, achieves $\mathcal{O}(N)$ scaling by diagonalizing the orthogonal TB-Hamiltonian approximately and is recognized as a fast and accurate model for atomic interaction [5–7]. It allows exploration of the dynamics of systems on macroscopic time and length scales on the atomic level that are beyond the realm of ab initio calculations. Such enhanced empirical TB based potentials make a sufficiently large number of particles and relaxation times up to µs accessible by MD including the electronic structure and the nature of the covalent bonds indirectly. The enhancement of the BOP is described in detail in [8–11] and summarized in Section 2. The ability of the BOP based MD is demonstrated here by comparing relaxations of quantum dots (cf. Section 3) and interface structures (cf. Section 4) with those using Tersoff potentials.

2. Analytic bond order potentials up to six moments

The approximations to develop analytic BOP potentials from DFT may be summarized by the following steps (for details cf. [5–7] and for the extensions cf. [8–11]): construct the TB matrix elements by Slater–Koster two-center integrals including s- and p- orbitals, transform the matrix to the bond representation, replace the diagonalization by Lanczos recursion, obtain the momenta from the continued fraction representation of the Green function up to order n for an analytic BOPn potential. The total cohesive potential energy U_{coh} has three contributions: pair repulsion, promotion energy U_{prom}, and bond energy as excess of the band energy over the individual atomic interactions $U_{\mathrm{bond}} = 2\sum_{i\alpha,j\beta}\Theta_{j\beta,i\alpha}H_{i\alpha,j\beta}$. In the BOP representation the matrix elements $H_{i\alpha,j\beta}$ are replaced by the Slater–Koster two-center integrals h_{ij} and the Goodwin–Skinner–Pettifor distance scaling function. The bond order $\Theta_{i\sigma,j\sigma}$ is equivalent to the electron density for which a concise analytical expression $\left[1+\dfrac{N^2(\Phi^i_{2\sigma}+\Phi^j_{2\sigma})+\Phi^i_{2\sigma}\Phi^j_{2\sigma}(2N+\triangle\Phi_{4\sigma})}{(N+\triangle\Phi_{4\sigma})^2}\right]^{-1/2}$ can be given that employs the normalized second and fourth moment $(\Phi_{2\sigma},\Phi_{4\sigma})$ of the local density of electronic states and $\triangle\Phi_{4\sigma}=(\Phi^i_{4\sigma}+\Phi^j_{4\sigma}-\Phi^{i2}_{2\sigma}-\Phi^{j2}_{2\sigma})/(\Phi^i_{2\sigma}+\Phi^j_{2\sigma})$, $N^2=\triangle\Phi_{4\sigma}+\Phi^i_{2\sigma}\Phi^j_{2\sigma}$. The normalized second moment was given as a sum of intersite and on-site hopping terms

$$\Phi^i_{2\sigma}=\sum_{k(i)\neq j} g_{\sigma jik}{}^2\hat{\beta}^2_{\sigma,ik}+\hat{\delta}^2_i \tag{1}$$

the latter being proportional to the energy splitting between atomic s- and p-states,

$$\hat{\delta}^2_i = p_{\sigma,i}(1-p_{\sigma,i})\,(E_{\mathrm{s}}-E_{\mathrm{p}})^2/\beta^2_{\sigma,ij} \tag{2}$$

* Extended contribution published at MMM2006 [1]

The contribution $\Phi_{4\sigma}$ to the 4th moment was given in terms of the matrix-elements of the tight binding Hamiltonian,

$$\Phi^i_{4\sigma} = \sum_{k(i)\neq j} \hat{\beta}^4_{ik} g^2_{jik} + \sum_{\substack{k(i)\neq j \\ l(k)\neq i,j}} \hat{\beta}^2_{ik}\hat{\beta}^2_{kl} g^2_{jik} g^2_{ikl} + \sum'_{k(i),l(i)\neq j} \hat{\beta}^2_{ik}\hat{\beta}^2_{il} g_{jik} g_{kil} g_{il} \quad (3)$$

with the bond angle θ_{jik}, the angular function

$$g_{\sigma,jik} = 1 + (\cos\theta_{jik} - 1)\, p_{\sigma,i} \quad (4)$$

reduced TB-parameters

$$p_{\sigma,i} = \frac{pp\sigma_{ii}}{|ss\sigma_{ii}| + pp\sigma_{ii}} \quad (5)$$

and normalized hopping integrals according $\hat{\beta}_{ik} = \beta_{ik}/\beta_{ij}$ etc. The resulting semi-empirical many body potential is transferable to describe phases and configurations not included in the parameter fit, a feature not found with other empirical potentials. Moreover, transferability extends to different kinds of materials, where only the parameter needs to be refitted. In the implementation of the enhanced BOP4+ [10, 11] a number of angular terms are included that are related to certain π bonds between neighboring atoms and contribute up to 40 %, but were neglected previously [8, 9]. Both contributions exhibit new angular dependencies, different from those already accounted for in the expressions given in [6] and the second order BOP2 [12, 13]. With the torsional function

$$g_{\varphi,jl} = p_{\pi,ik}\sqrt{p_{\sigma,i}p_{\sigma,k}}\cos\varphi_{jl}\sin\theta_{jik}\sin\theta_{ikl} \quad (6)$$

this contribution reads

$$\sum_{k(i)\neq j}\sum_{l(k)\neq i,j} \hat{\beta}^2_{\sigma,ik}\hat{\beta}^2_{\sigma,kl}\left[2g_{\sigma,jik}g_{\sigma,ikl} + g_{\varphi,jl}\right] g_{\varphi,jl} \quad (7)$$

Similarly on-site contributions to $\Phi_{4\sigma}$ proportional to the energy splitting δ_i are included:

$$\sum \hat{\beta}^2_{ik}\left\{g_{jik}(2\hat{\delta}^2_i + \hat{\delta}^2_k) + \hat{p}_i(1-\hat{p}_i)\,\hat{\delta}^2_i(1-\theta_{jik})^2\right\} + \hat{\delta}^4_i \quad (8)$$

The new terms (6), (7), and (8) provide a higher stiffness as will be demonstrated by the applications of Sections 3 and 4. The higher stiffness is the reason for the spontaneous dimer buckling of the Si[001] surface reconstruction, discussed in detail in [11] and not observed in previous BOP4 and Tersoff potentials. Besides an accurate fit, the BOP requires well parameterized TB matrix elements or parameter optimizing, and the problem of transferability has to be considered separately. For BOP of order $n = 2$ [12, 13] the bond-order term looks like a Tersoff potential and the numerical behavior of BOP2 and the empirical Tersoff potential are approximately equivalent. A detailed description of the enhanced analytical BOP4+ is given elsewhere [10, 11], together with the derivation of the individual terms and their importance to better describe the electronic origin for angular dependend bonding.

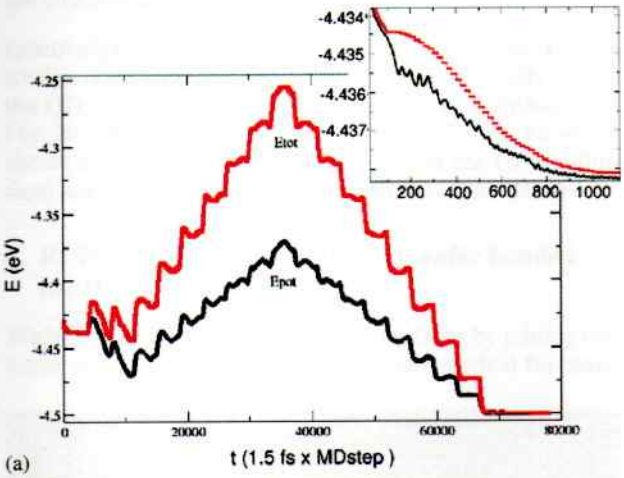

(a)

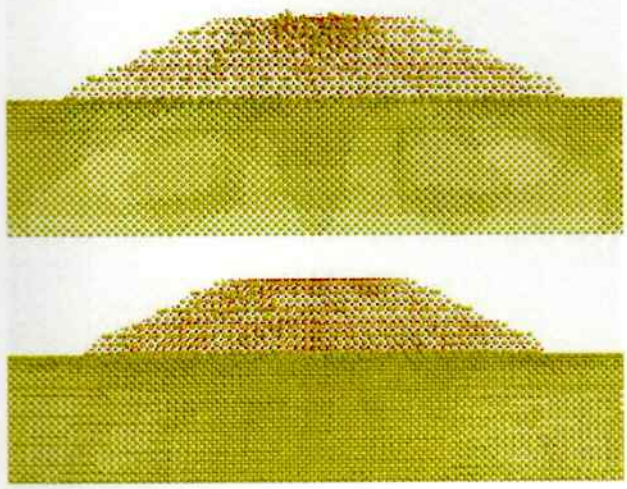

(b)

Fig. 1. MD relaxtion of an SiGe/Si island: (a) Potential and total energy during annaling up to 900 K, inset: enlarged first 1000 steps relaxing start configuration at 0 K, (b) [110] views after annealing with a Tersoff potential (top) and an analytical BOP4+ (bottom).

3. BOP4+ in MD relaxation of quantum dots

A quantum dot (QD) is a nanometer scaled island or region of suitable material free-standing on or embedded in semiconductor or other matrices. Shape, size and strain field of single QDs as well as quality, density, and homogeneity of equisized and equishaped dot arrangements are particularly important features which control the optical properties, the emission and absorption of light, the lasing efficiency, etc. MD with suitable potentials allows one to describe the relaxation and to predict structural properties of QDs.

Figure 1a shows the behavior of the potential and the total energy of an SiGe/Si-island and Fig. 1b the structural difference after relaxing the system up to 900 K with Tersoff and BOP4+ potentials. Due to the different nearest and next nearest neighbor relations, i.e. hopping matrix elements up to 6th order, the better stiffness of the BOP4+ yields better structural stability.

Figure 2a shows the difference in lattice plane bending comparing the atomic positions after annealing an embedded truncated (001)-SiGe/Si quantum dot of pyramidal shape having 111 faccettes. The different bending of the atomic rows is demonstrated using different colors for Si and Ge after applying the Tersoff potential (yellow/red, re-

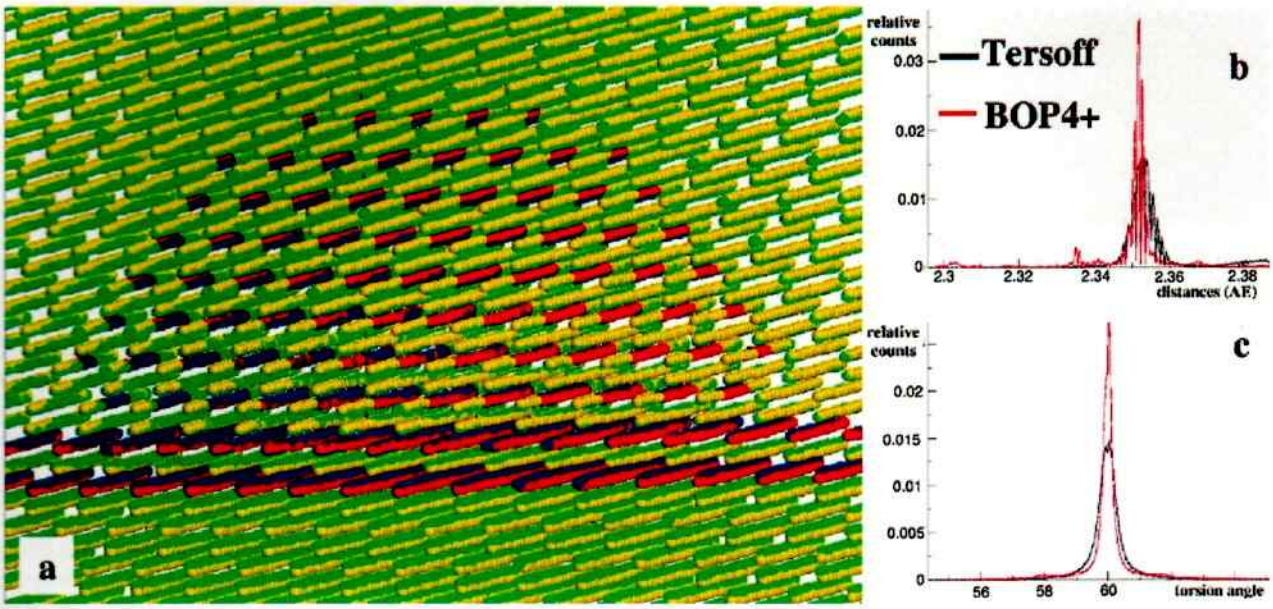

Fig. 2. MD relaxation up to 900 K of an embeded SiGe pyramid in Si comparing Tersoff and BOP4+ potentials: (a) Relaxed atom positions for Tersoff (Si yellow, Ge red) and BOP4+ (Si green, Ge blue) with a slight overall shift to separate the 110-dumbbell rows, (b) pairs distribution, and (c) distribution of the torsion angles.

spectively) and the enhanced BOP4+ (green/blue, respectively). Thus different strains are created especially within the QD, which is also reflected by the pair distribution in Fig. 2b. The torsion angle distribution in Fig. 2c, however, shows solely a sharper maximum around the 60° equilibrium angle indicating the higher stiffness of the BOP4+.

4. BOP4+ in MD investigations of wafer bonded interfaces

Wafer bonding, i. e. the creation of interfaces by joining two wafer surfaces, has become an attractive method for many practical applications in microelectronics, micromechanics or optoelectronics. The macroscopic properties of bonded materials are mainly determined by the atomic processes at the interfaces during the transition from adhesion to chemical bonding. Thus, the description of the atomic processes is of increasing interest to support the experimental investigations or to predict the bonding behavior. Whereas bonding of two perfectly aligned, identical wafers yields a single, perfectly bonded wafer without defects, miscut of the wafer results in steps on the wafer surfaces and thus edge dislocations at the bonded interfaces are created. Bonding wafers with rotational twist leads additionally to

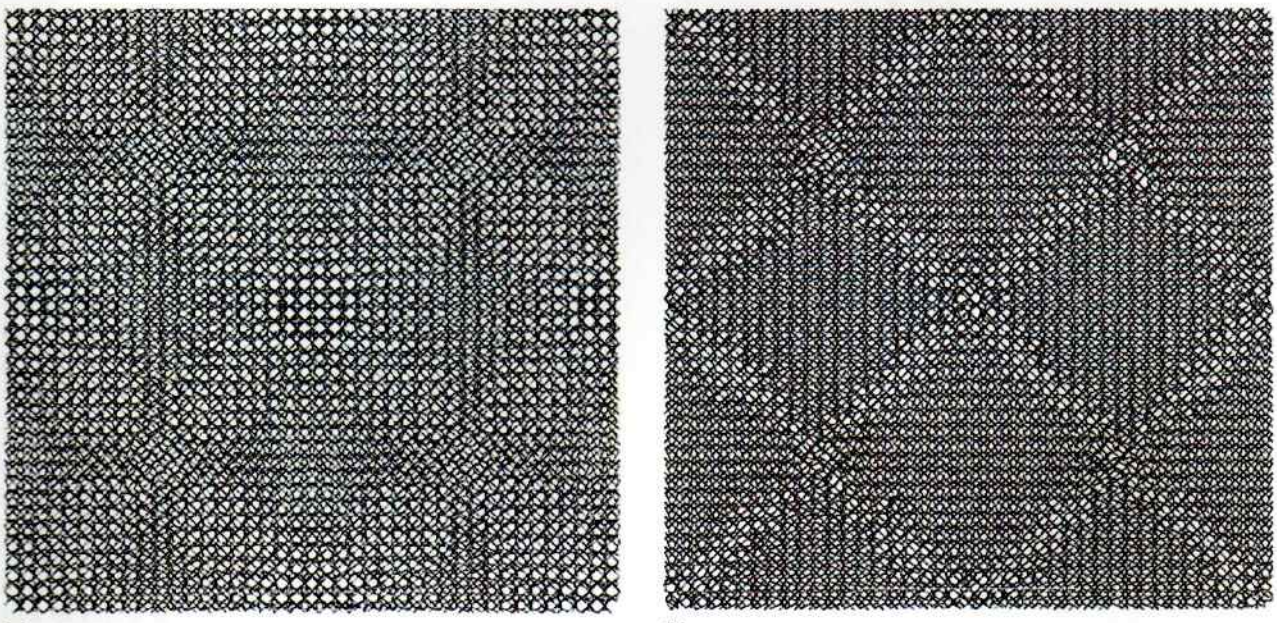

(a) (b)

Fig. 3. MD simulated structural models of bonded wafers ([001] views, bond representation of 3 lattice planes around the interface) with rotational 2.8° twist angles (134 500 atoms, 22 nm box) annealed at 900 K for orthogonal dimer start configurations: (a) Tersoff potential; (b) BOP4+ potential.

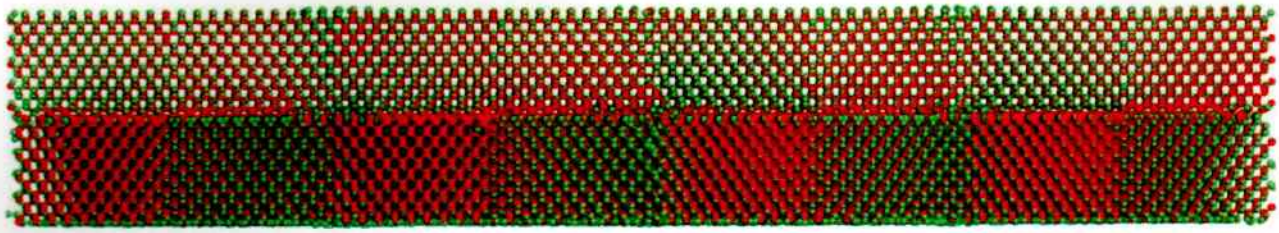

Fig. 4. MD relaxation of bonding rotationally twisted wafers ([110] view) with 2.8° angle, 22 nm box, orthogonal dimers: structural difference using Tersoff (green) and BOP4+ potentials (red).

a network of screw dislocations at the interface, depending on the twist angle different bonding behavior is observed as discussed in detail, for example, in [14]. A special situation is the 90° twist, for example between monoatomic steps, giving a (2×2) reconstructed interface and consisting of structural units called the $\bar{4}2$m-dreidl [15–17]. The dreidl structure is also found to be the minimum energy configuration in DFT-LDA simulations. The geometric arrangements of the interface defects fulfill the well-known rule to compensate the misfit. All local interface relaxations, however, are strongly influenced by the atomic potential model used, as it is demonstrated in Figs. 3–6 for the different core regions comparing MD interface simulations with Tersoff and BOP4+. Figures 3 and 4 show the resulting minimum structures gained for higher annealing temperatures (900 K) of a wafer bonded interface with a twist rotation of 2.8°. The [001]-projections of the bonds normal to the bonded interface up to next nearest neighbors is given in Fig. 3a and b for the MD relaxation with Tersoff and BOP4+ potentials, respectively. In Fig. 4 the [110] projection is shown, with both the Tersoff and the BOP4+ simulation projected by different colors into the same view. One reveals the more located, imperfectly bonded regions around the screw dislocations for the Tersoff potential, whereas the relaxation with BOP4+ yields more stability due to the higher potential stiffness according to the 6th moment hopping terms. Finally, in Fig. 5 the pair-, bond angle-, and torsion angle distributions are shown for the 2.8°-twist bonded interface, only 3 lattice planes around the interface are considered in distance and angle counting showing up the higher stiffness as the reason for the different core reconstructions. The Tersoff potential yields the characteristic first and second neighbor distances as well as the bond angle of 109°. The calculation with the BOP4+ demonstrates the characteristic deviations due to the better description of the electronic bond structure. So, for instance, the Tersoff potential is defined without torsion, thus the corresponding distribution in Fig. 5c has no relevant peaks. However, the angular distribution Fig. 5b shows remarkable maxima at 95° and 125°.

Figure 6 shows the interface region after bonding of 8.8° rotationally twisted (001)-Si wafers. The annealing at 900 K rearranges the atomic configurations at the interfaces to screw dislocations with overlapping core regions, thus the atomic rows at the interface are bent nearly across the whole wafer. Contrary to the results for the 2.8° twist boundary, the peak of the pair distribution on the right hand side of Fig. 6 is sharpened for the BOP4+ potential. Thus here for the overlapping core regions of the screw dislocations the higher stiffness of the potential yields better relaxation of the bonded interface.

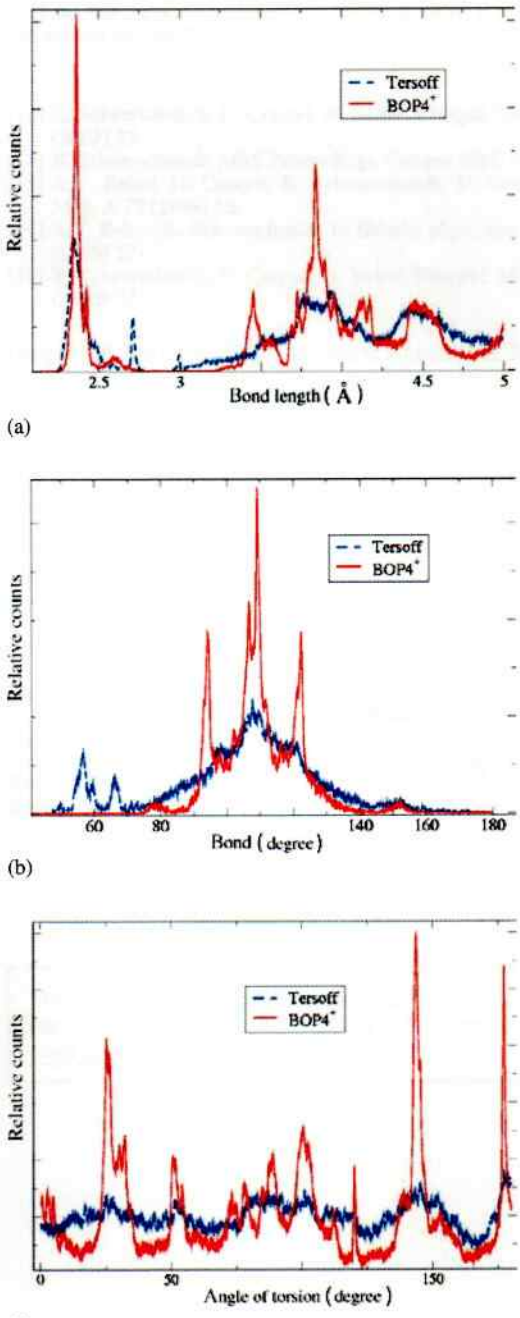

Fig. 5. Distribution functions for MD simulated structural models of bonded wafers with rotational twist angle of 2.8° annealed at 900 K assuming Tersoff potential (blue) and BOP4+ potential (red): (a) radial distribution function, (b) bond angles, and (c) torsion angles.

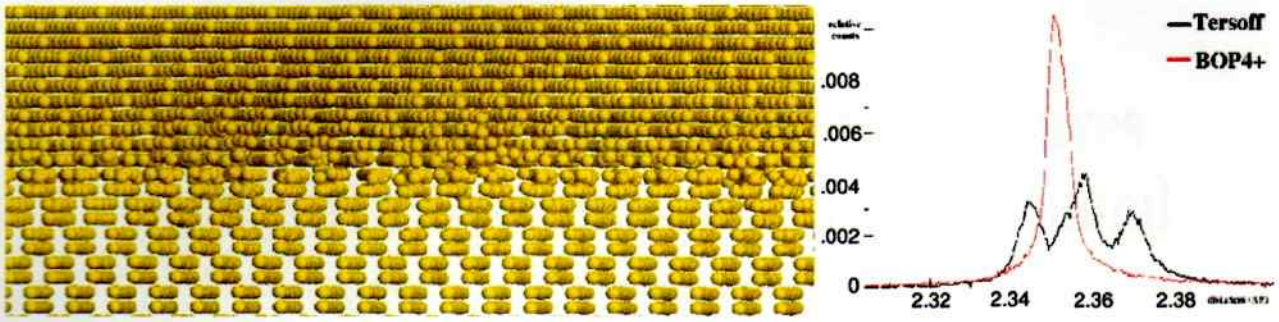

Fig. 6. MD relaxation of bonding rotationally twisted wafers with 8.8° angle, 11 nm box, orthogonal dimers: (a) Interface region in approximately [100] view of the lower crystal part, (b) pair distribution of five adjacent layers around the interface.

5. Conclusions

Molecular dynamics simulations (MD) based on empirical potentials are used to investigate the relaxation of nanostructures. It is demonstrated that different final structures for different potentials occur in simulating, for example, quantum dot relaxations or the bonding of two Si(001) wafers rotationally misaligned. The angular and distance behavior near defects shows the better electronic potential structure for the enhanced BOP4 potential. It clearly demonstrates the importance of enhanced empirical potentials as given by the tight-binding based analytic bond-order potential BOP4+ up to 6th order momenta.

References

[1] K. Scheerschmidt, V. Kuhlmann, in: P. Gumbsch (Ed.), Proc. Multiscale Materials Modelling, MMM2006, Freiburg, 18.–22. 9. 2006, 102–105.
[2] K. Scheerschmidt: Empirical Molecular Dynamics, in: D.A. Drabold, S. Estreicher (Eds.), Theory of Defects in Semiconductors, Topics in Applied Physics, Springer Verlag 2006, Chapter 9, 213–244.
[3] K. Scheerschmidt, P. Werner, in: M. Grundmann (Ed.), Nano-Optoelectronics: Concepts, Physics and Devices, Springer Verlag 2002, Chapter 3, 67–98.
[4] K. Scheerschmidt, V. Kuhlmann: Interface Sci. 12 (2004) 157.
[5] A.P. Horsfield, A.M. Bratkovsky, M. Fearn, D.G. Pettifor, M. Aoki: Phys. Rev. B 53 (1996) 12694.
[6] D.G. Pettifor, M.W. Finnis, D. Nguyen-Manh, D.A. Murdick, X.W. Zhou, H.N.G. Wadley: Mater. Sci. Eng. A 365 (2004) 2.
[7] M.W. Finnis: Interatomic Forces in Condensed Matter, Oxford Series on Materials Modelling, Oxford University Press 2003.
[8] R. Drautz, D.A. Murdick, D. Nguyen-Manh, X.W. Zhou, H.N.G. Wadley, D.G. Pettifor: Phys. Rev. B 72 (2005) 144105.
[9] D.G. Pettifor, I.I. Oleynik: Prog. Mater. Sci. 49 (2004) 285.
[10] V. Kuhlmann: Thesis, Martin-Luther-Universität, Halle 2006.
[11] V. Kuhlmann, K. Scheerschmidt: Phys. Rev. B 75 (2007) 014306.
[12] D. Conrad, K. Scheerschmidt: Phys. Rev. B 58 (1998) 4538.
[13] K. Scheerschmidt, D. Conrad, A. Belov: Comput. Mater. Sci. 24 (2002) 33.
[14] K. Scheerschmidt: MRS Proceedings Volume 681E (2002) I2.3.
[15] A.Y. Belov, D. Conrad, K. Scheerschmidt, U. Gösele: Philos. Mag. A 77 (1998) 55.
[16] A.Y. Belov, K. Scheerschmidt, U. Gösele: phys. stat. sol. (a) 159 (1999) 171.
[17] K. Scheerschmidt, D. Conrad, A. Belov: Comput. Mater. Sci. 24 (2002) 33.

(Received April 19, 2007; accepted August 10, 2007)

Bibliography

DOI 10.3139/146.101574
Int. J. Mat. Res. (formerly Z. Metallkd.)
98 (2007) 11; page 1081–1085

ISSN 1862-5282

Correspondence address

Dr. Kurt Scheerschmidt
Max Planck Institute of Microstructure Physics
Weinberg 2, D-06120 Halle, Germany
Tel.: +49 345 558 2910
Fax: +49 345 551 1223
E-mail: schee@mpi-halle.de

You will find the article and additional material by entering the document number MK101574 on our website at www.ijmr.de